

DTIC FILE COPY

AEOSR-TR- 90 0013

(2)

PSI-1006/TR-855

AD-A226 768

ROTATIONAL ENERGY TRANSFER IN METASTABLE STATES OF
HETERONUCLEAR MOLECULES

Interim Report

S.J. Davis

Physical Sciences Inc.
Research Park, P.O. Box 3100
Andover, MA 01810

January 1989

Unclassified

Air Force Office of Scientific Research (AFOSR)
Building 410
Bolling AFB, DC 20332-6448

IC
ECTE
SEP 27 1990
E D

DISTRIBUTION STATEMENT A

Approved for public release;
Distribution Unlimited

90 00 25 276

Unclassified

SECURITY CLASSIFICATION OF THIS PAGE

REPORT DOCUMENTATION PAGE

1a. REPORT SECURITY CLASSIFICATION Unclassified			1b. RESTRICTIVE MARKINGS		
2a. SECURITY CLASSIFICATION AUTHORITY			3. DISTRIBUTION / AVAILABILITY OF REPORT unlimited		
2b. DECLASSIFICATION / DOWNGRADING SCHEDULE					
4. PERFORMING ORGANIZATION REPORT NUMBER(S) PSI-1006/TR-855			5. MONITORING ORGANIZATION REPORT NUMBER(S) AFOSR-TR- 80 0913		
6a. NAME OF PERFORMING ORGANIZATION Physical Sciences Inc.		6b. OFFICE SYMBOL (if applicable)		7a. NAME OF MONITORING ORGANIZATION AFOSR	
6c. ADDRESS (City, State, and ZIP Code) P.O. Box 3100 Andover, MA 01810			7b. ADDRESS (City, State, and ZIP Code) Bldg 410 Bolling AFB DC 20332-6448		
8a. NAME OF FUNDING / SPONSORING ORGANIZATION AFOSR		8b. OFFICE SYMBOL (if applicable) NC		9. PROCUREMENT INSTRUMENT IDENTIFICATION NUMBER F49620-86-C-0061	
8c. ADDRESS (City, State, and ZIP Code) Building 410 Bolling AFB, DC 20332-6448			10. SOURCE OF FUNDING NUMBERS		
PROGRAM ELEMENT NO. 61102F		PROJECT NO. 2303		TASK NO. B1	
WORK UNIT ACCESSION NO.					
11. TITLE (Include Security Classification) Rotational Energy Transfer in Metastable States of Heteronuclear Molecules					
12. PERSONAL AUTHOR(S) S.J. Davis					
13a. TYPE OF REPORT Interim		13b. TIME COVERED FROM 6/27/88 TO 12/26/88		14. DATE OF REPORT (Year, Month, Day) 1/23/89	
15. PAGE COUNT 31					
16. SUPPLEMENTARY NOTATION					
17. COSATI CODES			18. SUBJECT TERMS (Continue on reverse if necessary and identify by block number)		
FIELD	GROUP	SUB-GROUP	Energy transfer, rotational-translational transfer, interhalogen molecules. (JS)		
19. ABSTRACT (Continue on reverse if necessary and identify by block number) The objective of this program is to measure and interpret state-to-state R-T transfer rate coefficients for selected interhalogen molecules. Spectrally resolved CW laser-induced fluorescence is the experimental method being used. A CW dye laser excites pure quantum states. The resolved fluorescence of the laser-excited level and the collisionally populated J' levels are analyzed. We have determined nearly 1000 state-to-state rate coefficients for R-T transfer in IF(B). Collision partners include He, Ne, Ar, Kr, Xe, N ₂ , and CF ₄ . Rate coefficients have also been determined for several initially excited J': 13, 27, 35 and 72. We have also investigated R-T transfer during vibrationally inelastic collisions. In addition, we have measured R-T rate coefficients in ICl(B). Finally, we have made preliminary comparisons of our R-T rate coefficients to several models that have been developed to predict R-T rate coefficient scaling as a function of ΔJ .					
20. DISTRIBUTION / AVAILABILITY OF ABSTRACT <input checked="" type="checkbox"/> UNCLASSIFIED/UNLIMITED <input type="checkbox"/> SAME AS RPT <input type="checkbox"/> DTIC USERS			21. ABSTRACT SECURITY CLASSIFICATION Unclassified		
22a. NAME OF RESPONSIBLE INDIVIDUAL Dr. Francis J. Wodarczyk			22b. TELEPHONE (Include Area Code) 202-767-4960		22c. OFFICE SYMBOL NC

DD FORM 1473, 84 MAR

83 APR edition may be used until exhausted.

All other editions are obsolete.

Unclassified

SECURITY CLASSIFICATION OF THIS PAGE

INTERIM PROJECT SUMMARY



1. TITLE: Rotational Energy Transfer in Metastable States of Heteronuclear Molecules
2. PRINCIPAL INVESTIGATOR: Dr. Steven J. Davis
3. INCLUSIVE DATES: 27 June 1988 - 26 December 1988
4. CONTRACT/GRANT NUMBER: F49620-86-C-0061
5. COSTS AND FY SOURCE: \$52,265 (FY88, 89)
6. SENIOR RESEARCH PERSONNEL: Dr. Steven J. Davis
7. JUNIOR RESEARCH PERSONNEL: Dr. Karl Holtzclaw
8. PUBLICATIONS: A-1
 1. "State-to-State Rotational Energy Transfer in IF $B^3\Pi(0^+)$ I. Collisions with He, Ne, Ar, Xe, N_2 , and CF_4 ," S.J. Davis and K. Holtzclaw (submitted to Journal of Chemical Physics).
 2. "State-to-State Rotational Energy in IF $B^3\Pi(0^+)$ II. Studies of Several Initially Populated Levels," S.J. Davis and K.W. Holtzclaw (to be submitted to Journal of Chemical Physics).
 3. "A Comparison of Rotational Energy Transfer in Homonuclear and Heteronuclear Halogen Molecules: A Case Study for $I_2(B)$ and IF(B)," S.J. Davis and K. Holtzclaw (to be submitted to Journal of Chemical Physics).
 4. "Application of Scaling Laws to R-T Transfer in IF(B)," S.J. Davis and K. Holtzclaw (manuscript in preparation).
9. ABSTRACT OF OBJECTIVES AND ACCOMPLISHMENTS:

A. Objectives

The objective of this project is to study rotational-to-translational (R-T) energy transfer in selected heteronuclear molecules. In particular, we are examining R-T transfer in the $B(^3\Pi_0^+)$ states of some halogen molecules, e.g., IF, ICl, and I_2 . We will also examine R-T transfer in the highly

metastable $A(^3\Pi_1)$ states of ICl. The experiments are conducted using a single frequency CW dye laser as the excitation source. With this laser, excited molecules in a pure quantum state (v' , J') can be produced. The resulting B \rightarrow X fluorescence is spectrally resolved and the rate coefficients for energy transfer are determined using a steady state kinetic analysis. In brief, the ratio of the fluorescence intensity from a collisionally populated satellite level (J_f) to that of a laser excited parent level (J_i) is directly proportional to the R-T rate coefficient, k_{if} . Knowledge of the radiative lifetime of the level J_f is required in the analysis, and the lifetimes of the states being investigated have been determined previously. The R-T rate coefficients are desired for two reasons. First, they will be used to test present theoretical scaling laws that predict the dependences of k_{if} upon J_i and upon the change in J (ΔJ) during a collision. These are of fundamental importance because the scaling laws depend upon the intermolecular potentials^{1,2}. Thus, fundamental insight is gained from these measurements. Secondly, these measurements have great practical relevance. Many of the species being investigated are excellent candidates for electronic transition chemical lasers. The degree of R-T relaxation in the excited state will in large measure determine the efficiency of the laser. Finally, knowledge of the R-T rates in the excited B-state is useful for estimating R-T relaxation in the ground state.

B. Progress

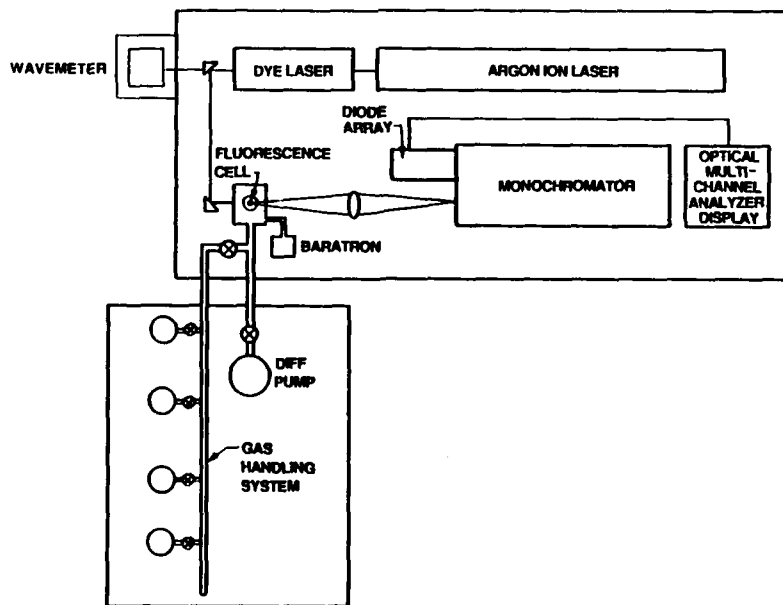
B.1 Introduction

In our annual report (July 1988)³ we presented rate coefficients for R-T transfer from several initially populated rotational levels in IF(B, $v'=6$) using the following collision partners: He, Ne, Ar, Kr, Xe, CF₄, and N₂. As part of our effort during the present reporting period, we have expended a considerable effort in interpreting these data. We have been able to gain insight into the physics of the interhalogen - rare gas R-T process and we have compared our data to several scaling laws that have been developed previously to systematize R-T in homonuclear molecules such as I₂ and Na₂.⁴ We have also

examined carefully the extent that multiple collisions might influence our results. Finally we have extended the experimental technique to ICl(B) and have determined preliminary sets of R-T rate coefficients for the collision partners He and Ar. Each of these topics is covered in the following sections.

B.2 Apparatus

Most of the apparatus used was explained in detail in our previous reports and a detailed description is not repeated here. A block diagram of the apparatus is shown in Figure 1. The experiments described in this report were made possible by the addition of a CW ring dye laser (Coherent 699-05). The ring laser was pumped by an Ar⁺ laser (Coherent Innova 100-20 UV) using the 514.5 nm line. Six watts of pump laser power produced a dye laser output of approximately 800 mW at the center of the Rhodamine 590 dye curve. The ring laser was passively stabilized and had a linewidth of 20 MHz. Detection of the resolved laser-induced fluorescence was accomplished with an optical multi-channel analyzer.



A-4734a

Figure 1. Block Diagram of Apparatus

B.3 IF Studies

The dye laser was introduced into the reaction cell via a series of turning prisms and was collimated to a diameter of 2 mm within the cell. A photomultiplier tube (Hamamatsu R-955) was placed normal to the dye laser beam in order to monitor the relative LIF power. A narrow band pass filter, covering the spectral range 480 to 500 nm, was placed in front of the PMT to discriminate LIF due to IF(B \rightarrow X) emission from that of I₂(B \rightarrow X). Wavelength discrimination is facilitated by the fact that I₂(B \rightarrow X) emission is absent for $\lambda < 500$ nm while several strong IF bands fall in the spectral region of the filter. As we explain below, this proved to be an invaluable diagnostic.

The optical excitation of IF(B) is typically performed between 460 to 500 nm since the ($v' \leftarrow v''=0$) bands having the highest Franck Condon factors lie in this region.⁵ However, operation of the ring laser near 500 nm requires coumarin dyes such as coumarin 102 and a pump laser that produces ultraviolet to violet (350 to 410 nm) lines. The pump laser of choice for this application is a Kr⁺ laser. Alternatively one could use the 350 nm output of the Ar⁺ laser. However, UV operation of the Ar⁺ laser can significantly reduce the lifetime of the plasma tube. Consequently we dismissed this approach and chose instead a less conventional way to excite IF using the dye laser in the red spectral range (570 to 600 nm). Since the band origin of IF(B-X) lies at 527.6 nm, the ring laser output frequency could not be made sufficiently energetic to pump from $v''=0$ with a red dye, and if the ring laser fundamental was to be used, a second source of energy was required. This was supplied by the vibrationally hot fraction of the IF (X) produced in the reaction F+I₂. This reaction is known to produce nascent IF(X,v) population distribution that are highly non-thermal.^{6,7}

The reaction cell was identical to that described in our earlier report. Atomic fluorine was produced by passing CF₄ through a microwave discharge. The F atoms then were mixed with I₂ introduced through a ring injector.

B.4 R-T Transfer in ICl(B)

The ICl molecule was also investigated during this reporting period. The B-state of ICl presents an interesting contrast to IF since there are fewer stable v' levels in ICl(B) than in IF(B). This is best illustrated by the respective potential energy diagrams shown in Figure 2a and 2b. We note that while all $v' \leq 8$ are stable in IF(B), predissociation occurs in ICl(B) for $v' \geq 2$.⁸⁻¹⁰ This offers us the possibility of studying R-T transfer from J' levels at or near the predissociation energy. It will be interesting to examine the rate coefficients for R-T transfer in a system where the potential is so severely perturbed.

The ICl molecule also allows us to obtain a preliminary picture of the effect of polarity upon the R-T process. For example, we are determining rate coefficients for R-T transfer using the same collision partners as we did for IF. In addition since we can readily vary the ICl vapor pressure, we can also use the highly polar ICl molecule as a collision partner to study R-T transfer within ICl(B).

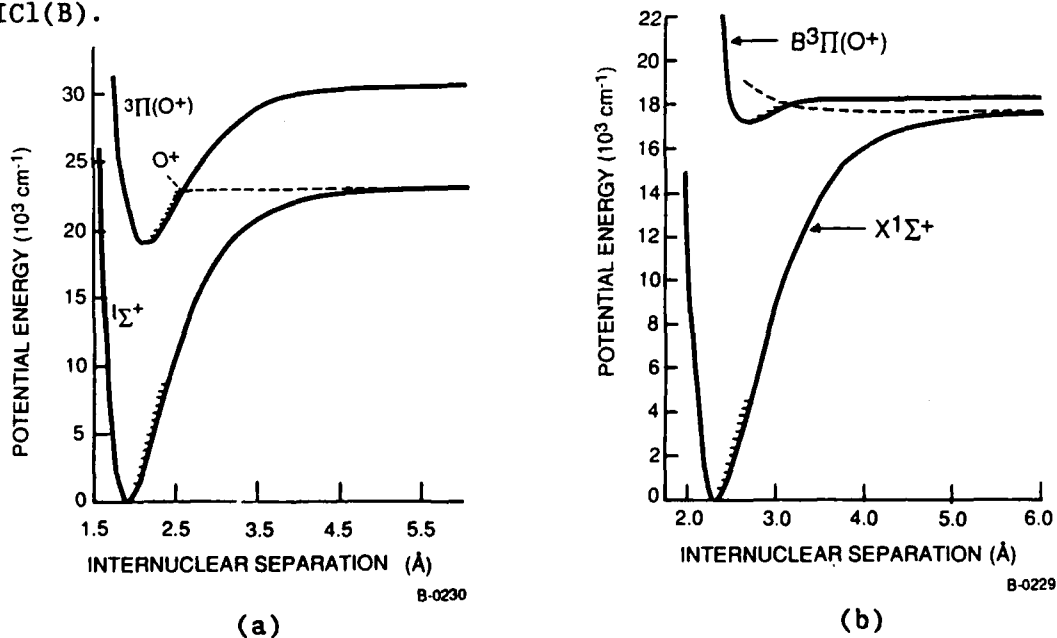


Figure 2. Potential Curves for IF and ICl. a) IF, b) ICl

To date we have extended our measurements to the B-state of ICl and have determined R-T rate coefficients for the collision partners helium and argon. These experiments were performed using the same methodology as in the IF studies. Initially, we chose ICl crystals as the source of ICl vapor since it is relatively easy to work with. However, I_2 contamination is a persistent problem in ICl and we actually began the experiments using ICl_3 as the source of ICl vapor. This provided a stable and clean flow of ICl that was almost free from I_2 .

These experiments were carried out by establishing a slow flow of ICl vapor through the loop injector formerly used for the I_2 in the IF studies. The ICl vapor pressure in the reaction cell was 10 mtorr. The bath gases were added as described previously³ and their pressures were measured with a Baratron capacitance manometer. We explored several J' levels and observed that the laser-induced fluorescence was surprisingly intense. For the preliminary results that we report here, the $v'=1$, $J'=40$ level was excited at 17043.4 cm^{-1} and the resolved fluorescence on the 1,8 band near 14450.0 cm^{-1} was recorded using the OMA system. Data analysis was identical to that employed for the IF experiments. The spectral fitting was accomplished using the spectroscopic constant of Clyne and McDermid.⁸

B.5 Scaling Law Tests

There are several motivations for developing and verifying scaling laws to describe R-T rate coefficients.^{1,2} Perhaps the most important reason is one of practicality; it is unrealistic to tabulate rate coefficients that describe all possible R-T processes even within one electronic state. The situation is drastically simplified if all R-T rate coefficients can be scaled to a few fundamental parameters. Indeed, the goal of this approach is to obtain a closed form expression that can be used to generate R-T rate coefficients. This would be particularly valuable in kinetic codes, e.g., chemical laser codes.

From a more fundamental perspective, there are also reasons for testing scaling laws. Some of the parameters in the scaling laws that have been developed can be related to physically meaningful quantities such as the interaction potentials. Consequently one can gain fundamental insight into some of the physics of the R-T collision.

There are several scaling laws that have been developed over the past two decades in order to predict all $k(i \rightarrow f)$ given that a few can be measured. For brevity we do not discuss the derivations of these scaling laws but instead we emphasize the important features of them and compare each to our data sets. There are two basic types of these laws: 1) those based upon the amount of energy exchanged and 2) those based upon the amount of angular momentum exchanged.

B.5.1 Energy Based Fitting Laws

The oldest and simplest fitting law is the exponential gap law given by Eq. (1)

$$\begin{array}{l} \text{EGL} \\ k(i \rightarrow f) = a e^{-(\Theta |\Delta E|)} \cdot R(\Delta E)(2J_f + 1) \end{array} \quad (1)$$

where a and Θ are fitting parameters and $R(\Delta E)$ is the ratio of the final density of translational states to the initial density of translational states. This form was developed by Polanyi and Woodall¹¹ in their studies of HF(v) relaxation and has been applied to a number of other species.

Pritchard and co-workers^{12,13} developed an alternate formalism that scaled the R-T rate coefficients to a power gap law given by Eq. (2)

$$\begin{array}{l} \text{SPGL} \\ k(i \rightarrow f) = a |\Delta E/B_v|^{-\alpha} \cdot N_\lambda(J_i, J_f)(R(\Delta E)) \end{array} \quad (2)$$

In Eq. (2) a , α , and λ are fitting parameters, B_v is the rotational constant, and N_λ is a factor that allows for a restriction on ΔM or a change in orientation of the molecule during the collision.

B.6 Angular Momentum Based Laws

The S-matrix formalism was applied to the R-T process by DePristo and co-workers¹⁴ and led to two scaling laws that have been successfully applied to R-T transfer in several homonuclear molecules such as I_2 and Na_2 . For illustration we present the expressions for these two scaling laws in Eqs. (3) and (4). The salient point is that the rate coefficient, $k(i \rightarrow f)$, for the R-T process $J_i \rightarrow J_f$ is expressed in terms of a basis rate coefficient $k(\ell \rightarrow 0)$. The infinite order sudden (IOS) law is given by

$$\begin{aligned}
 & \text{IOS} \\
 k(i \rightarrow f) = & (2 J_{f+1}) \exp[(E_{J_i} - E_{J_f})/kT] \\
 & \times \left[\sum_{\ell} \begin{pmatrix} j_i & \ell & j_f \\ 0 & 0 & 0 \end{pmatrix}^2 (2\ell+1) k(\ell \rightarrow 0) \right]
 \end{aligned} \tag{3}$$

where

$$j_{>} = \text{larger of } (j_i, j_f)$$

$$\begin{pmatrix} j_i & \ell & j_f \\ 0 & 0 & 0 \end{pmatrix} = 3j \text{ symbol}$$

and

$$k(\ell \rightarrow 0) = a[\ell(\ell+1)]^{-\gamma}.$$

The sum over ℓ is taken over $|j_i - j_f| \leq \ell \leq |j_i + j_f|$ and a and γ are the fitting parameters.

The underlying principle of the IOS approximation is that the R-T collision is essentially instantaneous and consequently the molecule cannot rotate during the collision. If the perhaps more realistic assumption is made that the collision does take a finite time, then additional terms are added to the IOS expression and we have the Energy Corrected Sudden law (ECS) given by Eq. (4)

$$k^{ECS}(j_i, j_f) = (2j_f + 1) \exp[(E_{j_i} - E_{j_f})/kT] \quad (4)$$

$$\times \left[\sum_{\ell} \begin{pmatrix} j_i & \ell & j_f \\ 0 & 0 & 0 \end{pmatrix}^2 (2\ell + 1) [A_{\ell}^{j_f}]^2 k(\ell \rightarrow 0) \right]$$

In Eq. (4)

$$A_{\ell}^{j_f} = \frac{1 + \tau_{\ell}^2/6}{1 + \tau_{j_f}^2/6}$$

where $\tau_{\ell} = 4\pi\ell_c \text{ cB}(j+1/2)/\bar{v}$. The parameter ℓ_c is interpreted on the collision length and \bar{v} is the mean relative velocity, and τ_{ℓ} is an effective collision time. Since ℓ_c is a fitting parameter, we see how this law can give some physical insight into the R-T process.

B.7 Results

a) Multiple Collision Analysis

We have discussed previously the kinetic analysis used to extract rate coefficients from the observed intensities of the initially populated (J_i) and collisionally populated (J_f) lines. In brief, a spectral fitting code provides

the population ratio $[N_f]/[N_i]$. In a purely single collision regime, this ratio is directly proportional to the R-T rate coefficient $k(i \rightarrow f)$:

$$[N_f]/[N_i] = k(J_i \rightarrow J_f)[M] \tau_R \quad (5)$$

where $[M]$ = number density of the bath gas and τ_R is the radiative lifetime of J_f . Consequently, a plot of $[N_f]/[N_i]$ versus $([M] \tau_R)$ should yield $k(J_i \rightarrow J_f)$. However, if the number density of M is too high, secondary collisions can occur and Eq. (5) is no longer an adequate description. The treatment of multiple collisions can take on varying levels of complexity and indeed can become computationally unwieldy. Ideally one would always work at pressures, sufficiently low, so that the probability of two or more collisions during one radiative lifetime is negligible. Unfortunately, these conditions are not always compatible with an adequate signal strength, and the possibility of multiple scattering must be considered. For IF(B), a bath gas pressure of approximately 25 mtorr would cause one collision per lifetime assuming a gas kinetic collision cross section. We obtained most of our data at pressures lower than this but, nevertheless, we wished to explore the effect of multiple collisions.

Secondary collisions have the effect of shortening the lifetime of the final state, J_f . The first order correction is accomplished by accounting for non-R-T processes such as collisional quenching of J_f , collisional predissociation of J_f , and V-T removal from V_i . Consideration of these effects leads to Eq. (6)

$$[N_f]/[N_i] = \frac{k(i \rightarrow f)[M] \tau_R}{1 + (k_Q[M] + k_p[M] + k_v[M])\tau_R} \quad (6)$$

where k_Q , k_p , and k_v are the respective rate coefficients for electronic quenching, predissociation, and V-T transfer. Note that all removal processes refer to the final J' level. From Eq. (2) we observe that a plot of

$[N_{J'}]/[N_{J'=72}]$ versus $[M]$ can be used to determine k_R if τ_R , k_Q , k_p , and k_v are known. For many of the interhalogens, all of these values are known, and in the case of IF(B), the term $(k_Q + k_p + k_v)[M]\tau_R$ is less than 0.1 for all $[M]$ used. Thus it is a small correction.

The next level of approximation allows for R-T removal from J_f to all other rotational levels within v_i . This treatment, first described by Steinfeld and Klemperer¹⁵ in their pioneering I_2 studies, yields Eq. (7)

$$[N_f]/[N_i] = \frac{k(i \rightarrow f) [M] \tau_R}{1 + \underbrace{\left(k_R^T [M] + k_v [M] + k_p [M] + k_Q [M] \right) \tau_R}_{\alpha}} \quad (7)$$

where

k_R^T \equiv total rate coefficient for R-T transfer from J_f to all other J within v_i .

This should be considered a first order correction since it does not allow for the important channel of repopulation of J_f via secondary collision from intermediate rotational levels exclusive of J_i . Note the ratio $[N_f]/[N_i]$ is linear in pressure only when the term α can be neglected. If we call these levels J_l , then we find that the term α becomes

$$\alpha = \left(k_R^T [M] - \sum_l k(J_l \rightarrow J_f) \frac{[N_l]}{[N_f]} [M] + k_v [M] + k_Q [M] \right) \tau_R \quad (8)$$

where $l \neq i$.

This additional term has the effect of counteracting the removal of J_f via the $k_T^R[M]$ term. In practice, multiple collisions are treated using Eq. (9) in an iterative fashion

$$[N_f]/[N_i](1+\alpha) = k(i \rightarrow f) [M] \tau_R \quad . \quad (9)$$

First, one examines plots of $[N_f]/[N_i]$ versus $[M]$ at the lowest attainable $[M]$ and extrapolates a linear slope. If this is done for each J_f , then a first order set of $k(i \rightarrow f)$ can be obtained. Using these $k(i \rightarrow f)$, one calculates α and modifies $[N_f]/[N_i]$. New $k(i \rightarrow f)$ are obtained and compared to the original $k(i \rightarrow f)$. The process is repeated until the $k(i \rightarrow f)$ converge. Several groups have used this approach when $|\Delta J| \lesssim 15$, e.g., Li_2 ,¹⁶ and OH .¹⁷ Even though our Stern-Volmer plots displayed little discernable curvature, we constructed a code to treat the corrections, through one iteration, using Eq. (9). After one iteration, this treatment resulted in large corrections ($> 50\%$) being indicated for the $\{K_{72,J}\}$ produced with the single collision analysis. It was clear that many iterations would have to be performed in order to arrive at a converged set of rate constants. We concluded that in IF(B) where $|\Delta J| \lesssim 80$, the iterative treatment introduces large uncertainties ($> 50\%$). A large portion of the uncertainties arises from the need to determine $[N_i]/[N_f]$ for each iteration. This approach appeared to be very laborious and impractical. Rather, we performed several tests to examine the potential problem of multiple collisions. First, examination of plots of $[N_f]/[N_i]$ versus $[M]$ were linear within approximately ± 10 percent for pressures up to 20 mtorr for all gases studied. For the case of $J_i=72$ we also carefully examined the populations of $J_f \leq 19$ as a function of $[M]$. We chose this region since it represented an exchange of rotational energy of nearly 5 kT (at 300 K) and two consecutive collisions would manifest as a quadratic dependence upon $[M]$. In all cases we observed a linear dependence of $[J_f^{19}]/[J_i]$ upon $[M]$ for pressures < 20 mtorr. At higher pressures a non-linear behavior was observed. This is illustrated for Ar in Figure 3. From similar plots we empirically determined pressures

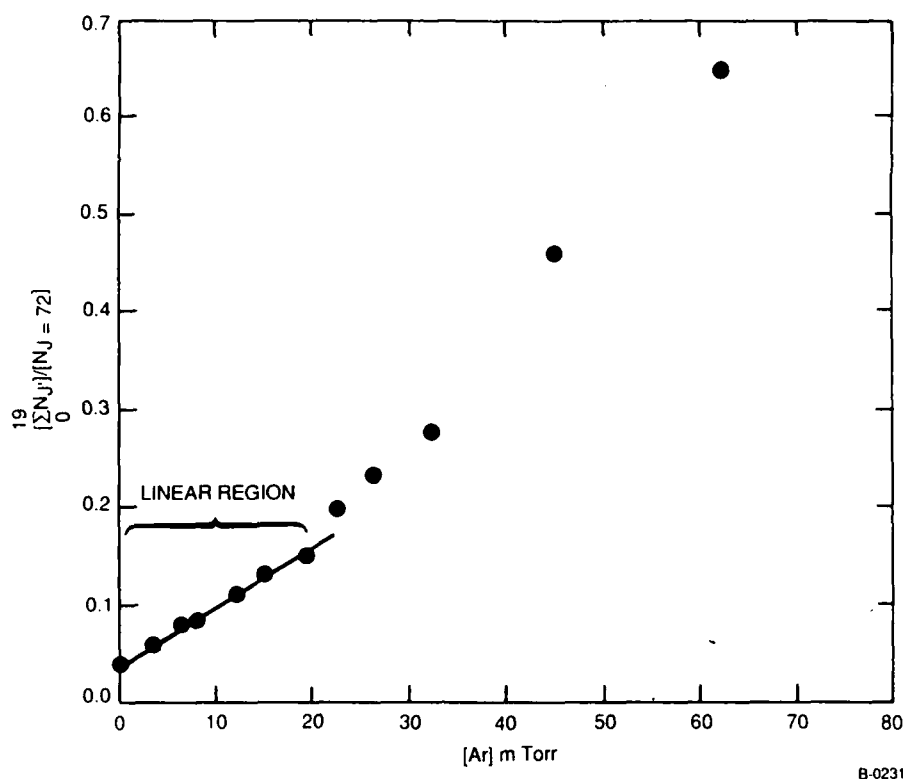
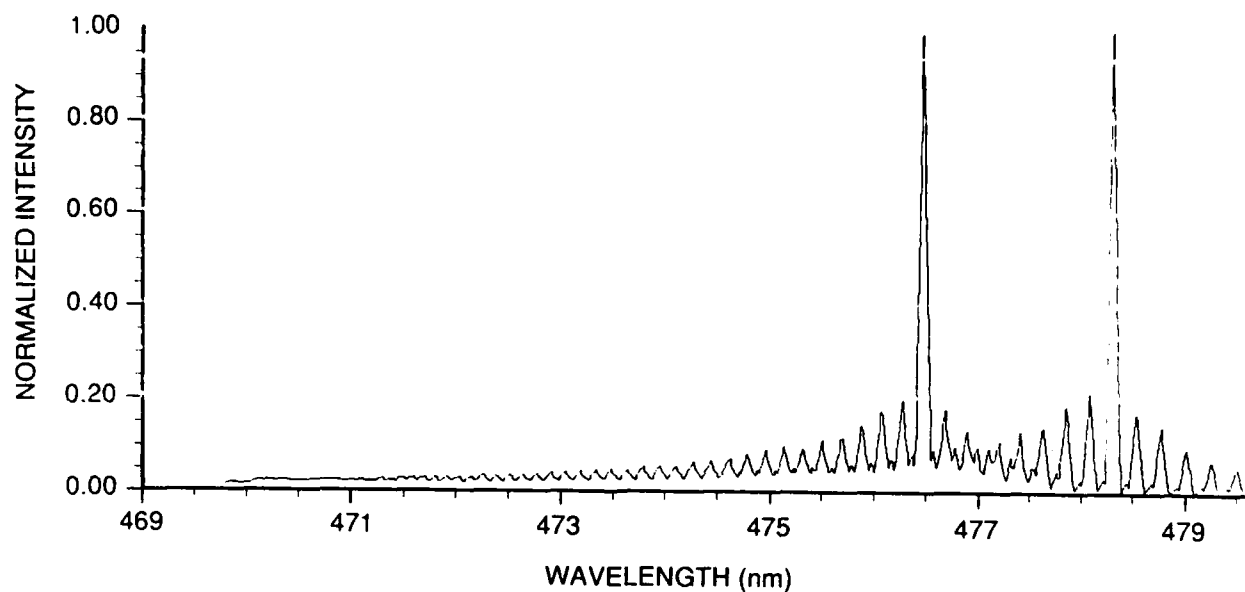


Figure 3. Stern-Volmer Plot of $[\sum N_J]/[N_J=72]$ Versus $[Ar]$. Note linear behavior for pressure less than 20 mtorr

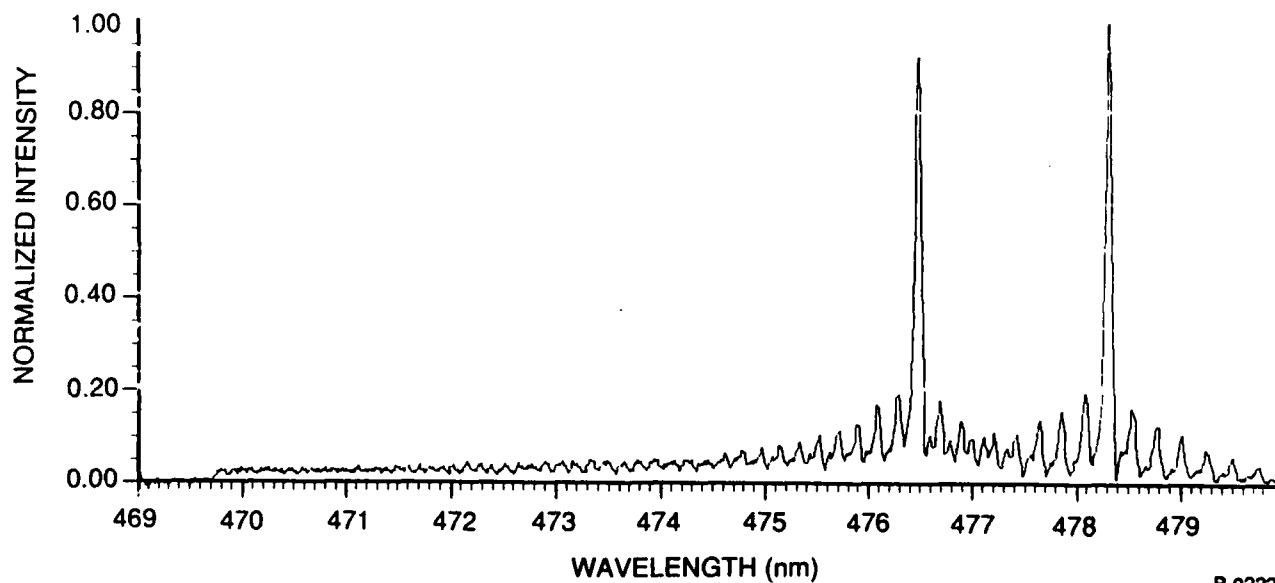
below which the dependence was linear. All analyses were completed using only those data with $[M]$ below these "critical" pressures.

We also performed one other test to determine whether our (essentially) single collision model was adequate. Using our matrix of $k(72 \rightarrow f)$ we predicted spectra as a function of $[M]$ using the single collision model. In Figure 4 we show a comparison of a predicted and actual spectrum using He at the relatively high pressure of 34 mtorr. The agreement is excellent, supporting our contention that multiple collision effects are essentially negligible. It appears that if multiple collisions are taking place, the depopulation of J_f is balanced by repopulation of the level from nearby levels. We cannot discern the difference between these two cases. However, in our analysis these are identical descriptions.



B-0221

(a)



B-0222

(b)

Figure 4. a) Synthetic Spectrum Produced by Assuming Single Collision Model and Measured Rate Coefficients for He. Calculation Run at $[\text{He}] = 34 \text{ mTorr}$. b) Resolved LIF Data for He at 34 mTorr .

b) Systematic Examination of the IF RET Cross Sections

The R-T cross section is a more fundamental parameter than the rate coefficient. While we cannot determine velocity dependent cross sections from our data we can calculate velocity independent cross sections $\sigma(i \rightarrow f)$ from Eq. (10)

$$\langle \sigma(i \rightarrow f) \rangle = \frac{k(i \rightarrow f)}{v} \quad (10)$$

where v is the center of mass velocity of IF+M. Of course in Eq. (10) we tacitly assume that $k(i \rightarrow f)$ is essentially independent of v . In Table 1 we present the total R-T cross sections ($\sum_f \sigma(i \rightarrow f)$) for He, Ne, Ar, Kr, Xe, N₂, and CF₄.

Table 1. Rate Coefficients and Velocity Independent Cross Sections for Total R-T Removal From J_i=72

Collision Partner	Rate Coefficient 10 ⁻¹⁰ cm ³ mol ⁻¹ s ⁻¹	Cross Section (10 ⁻¹⁶ cm ²)
Helium	2.94	23.1
Neon	2.29	38.3
Argon	2.16	48.1
Krypton	1.92	55.7
Xenon	2.15	71.1
N ₂	3.69	71.1
CF ₄	2.42	60.7

It is also instructive to examine the mass dependence of these cross sections. From classical mechanics it can be shown that the angular momentum exchanged in an IF+M encounter is

$$L = r \times p \quad . \quad (11)$$

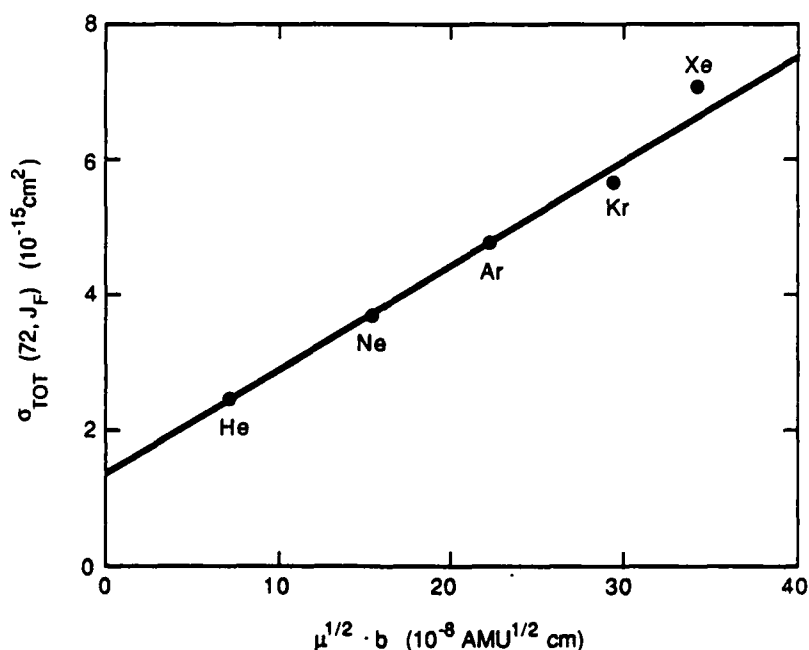
If we assume that the collision plane is normal to the rotation axis, then

$$L = \mu v b \quad (12)$$

where μ is the reduced mass, v is the rms center of mass velocity, and b is the impact parameter. Using $v = (8k T / \Pi \mu)^{1/2}$, we find that

$$L \propto \mu^{1/2} b \quad . \quad (13)$$

Hence a heavier collision partner is expected to exchange more angular momentum per collision. In Figure 5 we plot the total R-T cross section for removal from $J_i=72$ for the collision partners He, Ne, Ar, Kr, and Xe. The abscissa in Figure 5 is the product $\mu^{1/2} b$ where we use the hard sphere



A-9969

Figure 5. Plot of σ_{TOT} Versus the Product of $b \times (\text{reduced mass})^{1/2}$ of the Collision System for $J_i=72$

diameter for b. The plot is consistent with our rather simple hard sphere model and clearly shows that the total R-T cross section increases as the mass of the collision partner is increased.

It is also relevant to examine the state-resolved cross sections and these are presented in Figure 6(a-d). These data indicates that the cross sections for small ΔJ are comparable for He, Ne, Ar, and Xe while those for large ΔJ increase dramatically as the mass of the collision partner is increased. From this comparison we conclude that the increase in the total R-T cross section as a function of collision partner mass is due predominately to large ΔJ being a much more probable event with the heavier partners.

Similar plots for Kr, N_2 , and CF_4 are shown in Figure 7(a-c). The CF_4 data shown in Figure 7 shows that a polyatomic collision partner behaves very differently from an atomic partner. The individual R-T cross sections are nearly uniform over a large range of ΔJ ; perhaps indicating that the internal degrees of freedom on CF_4 are efficient acceptors of the rotational energy of IF.

C. ICl Results

A sample spectrally resolved $ICl(B \rightarrow X)$ fluorescence spectrum and the corresponding spectral fit is shown in Figure 8 using Ar bath gas. Using the kinetic scheme described earlier, we determined the population ratio $[N_f]/[N_i]$ and a typical Stern-Volmer lot is shown in Figure 9. Although these are the first ICl data, the scatter is not prohibitive and we have been able to obtain preliminary values for $k(i \rightarrow f)$ for $J_i=40$ using Ar and He. These data are presented in Figures 10 and 11. Examination of these plots shows that as ΔJ increases, the $k(i \rightarrow f)$ drop more rapidly for He than they do for Ar. This is similar to the IF results. We will put these results on a more quantitative basis during the next few months.

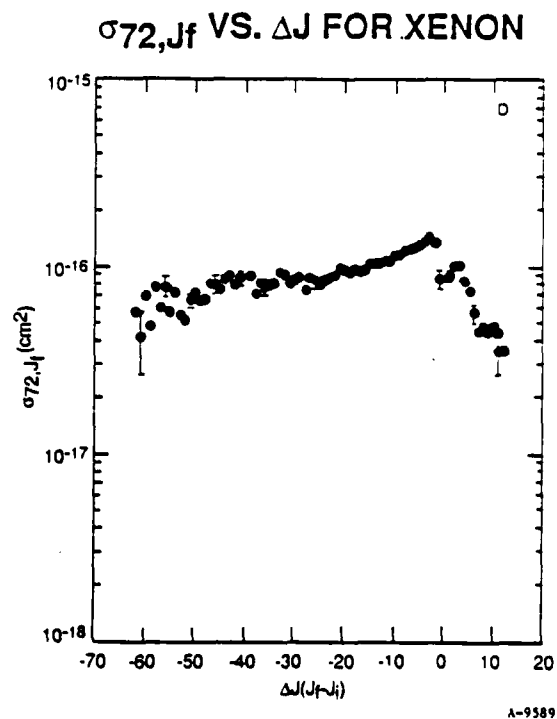
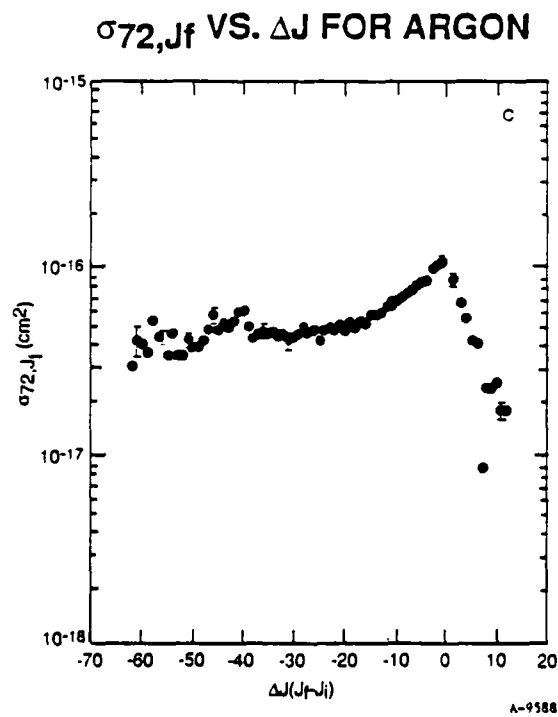
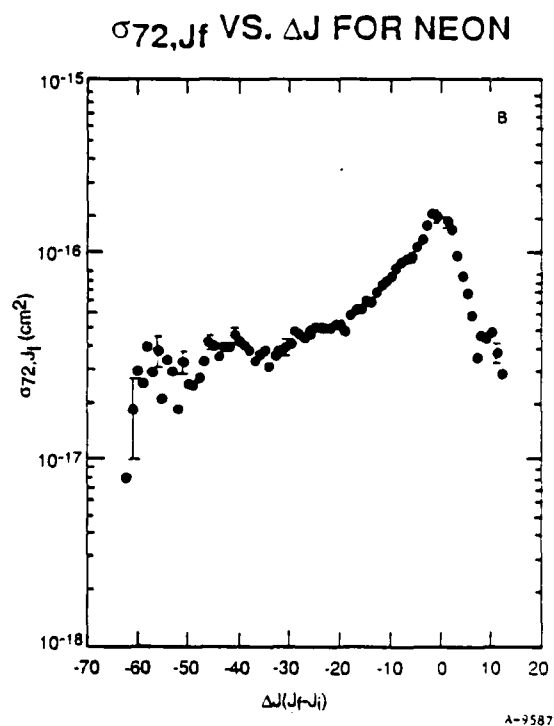
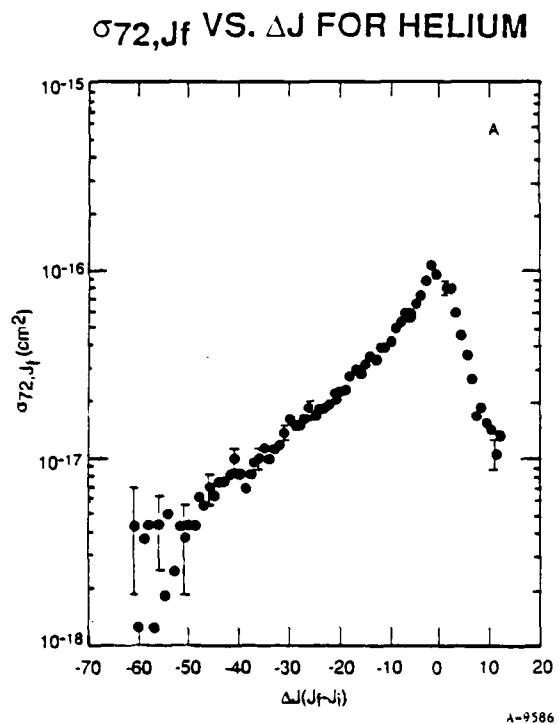
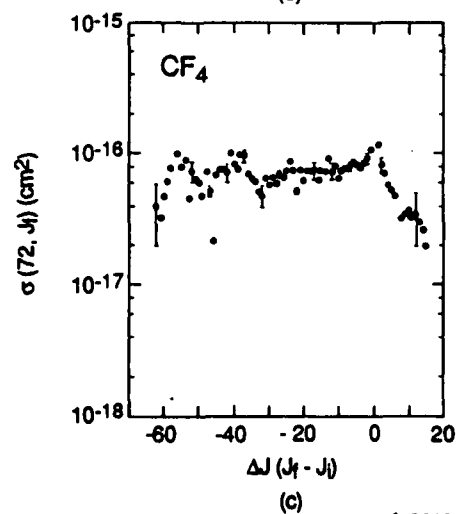
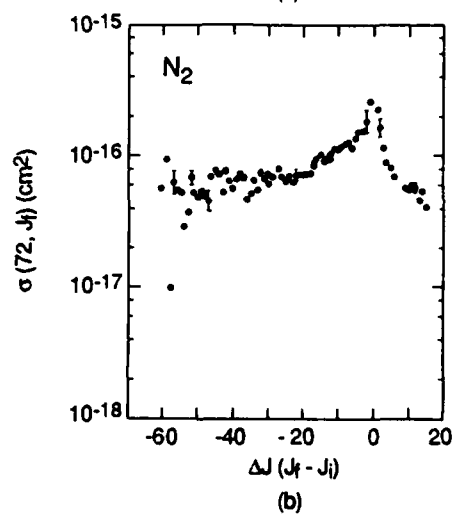
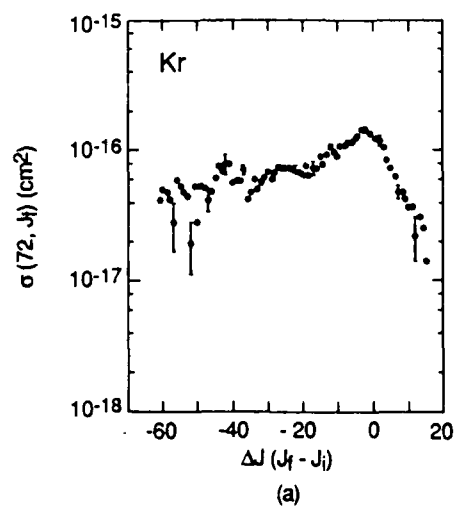
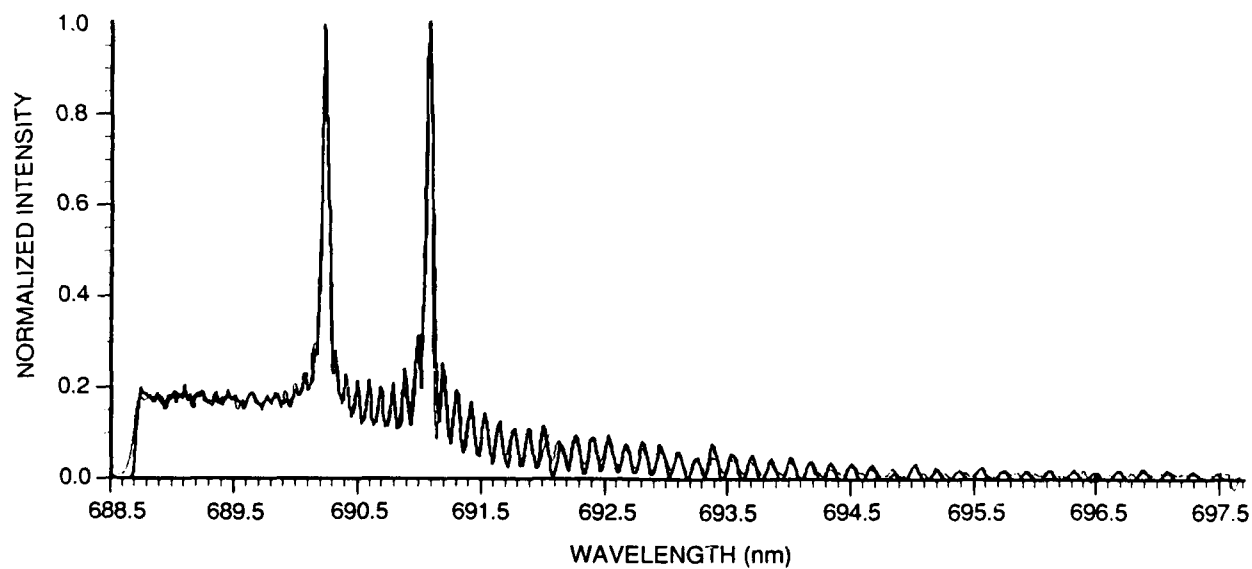


Figure 6. State-to-State Cross Sections for He, Ne, Ar, and Xe



A-9897

Figure 7. State-to-State Cross Sections for Kr, N_2 , and CF_4



B-0299

Figure 8. Resolved Fluorescence for $\text{ICl(B)} + \text{Ar}$, $J_i=40$
Argon pressure was 60 mtorr

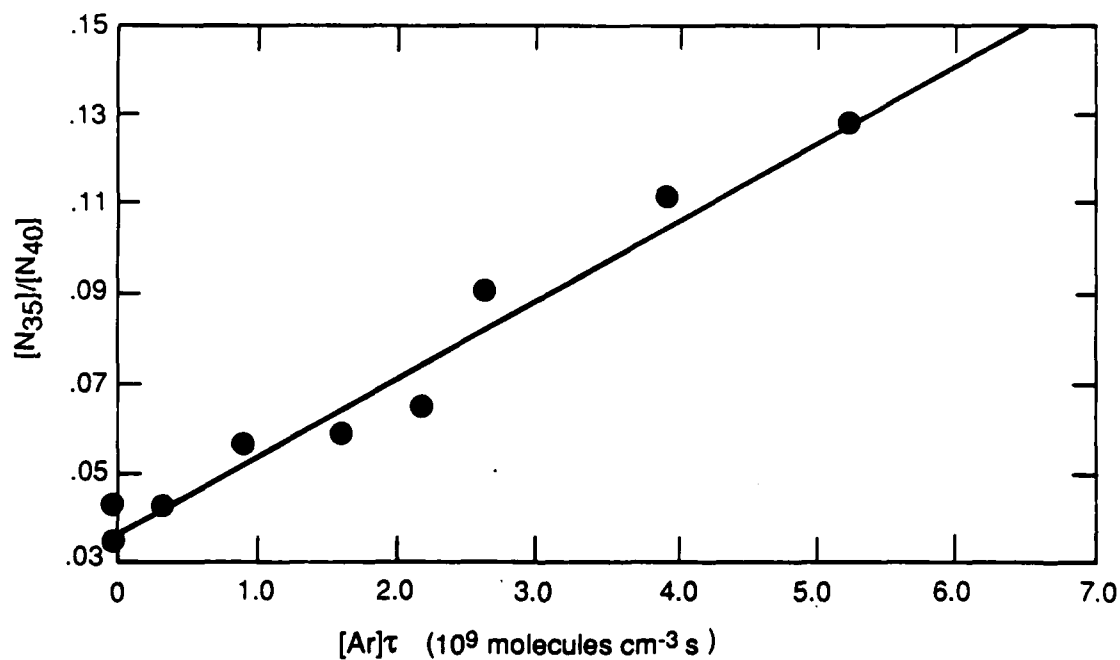
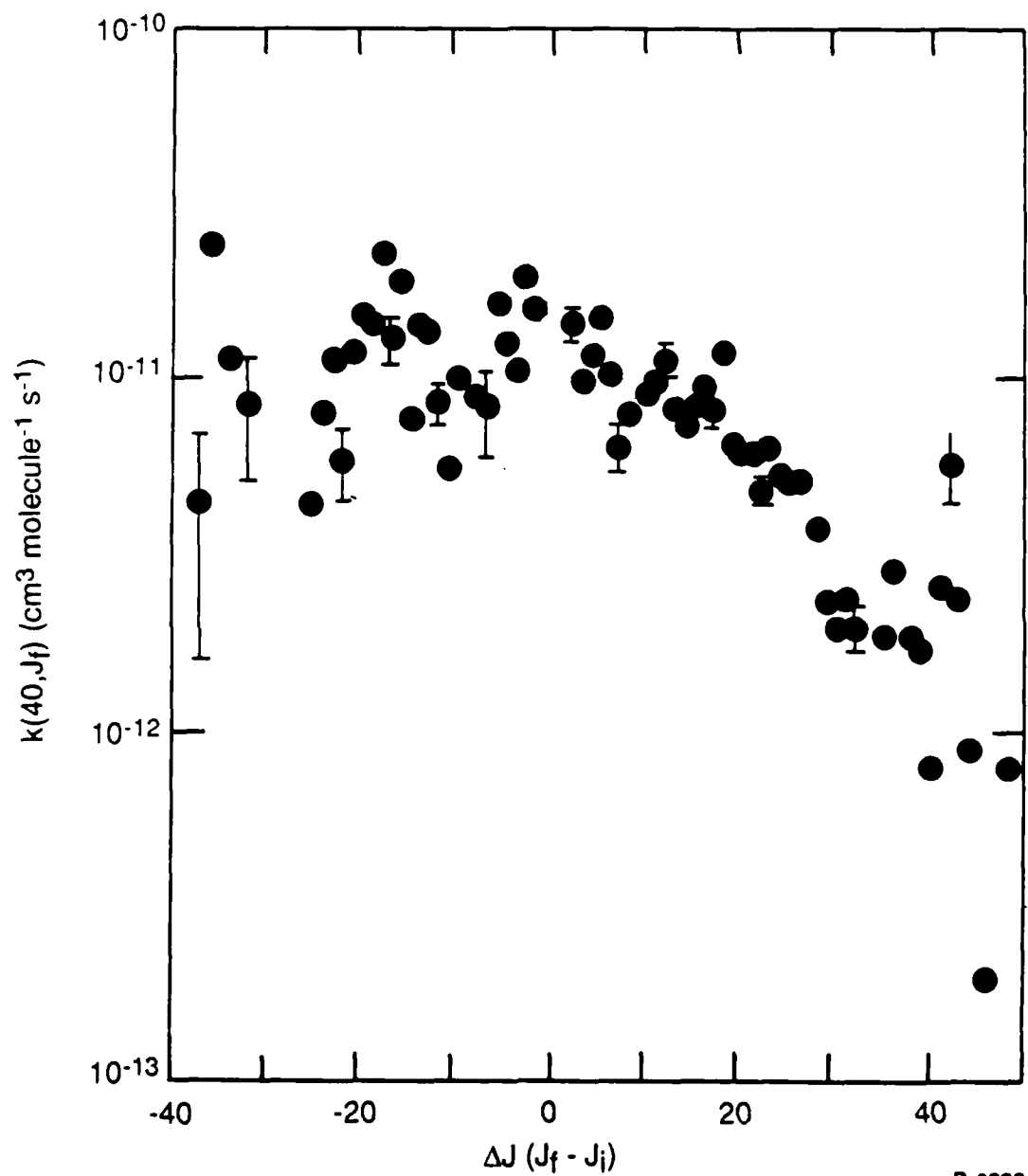


Figure 9. Stern-Volmer Plot for $\text{ICl(B)} + \text{Ar}$, $J_f=35$



B-0233

Figure 10. Preliminary Matrix of R-T Rate Coefficient for
 $\text{ICl} + \text{Ar}, J_i = 40$

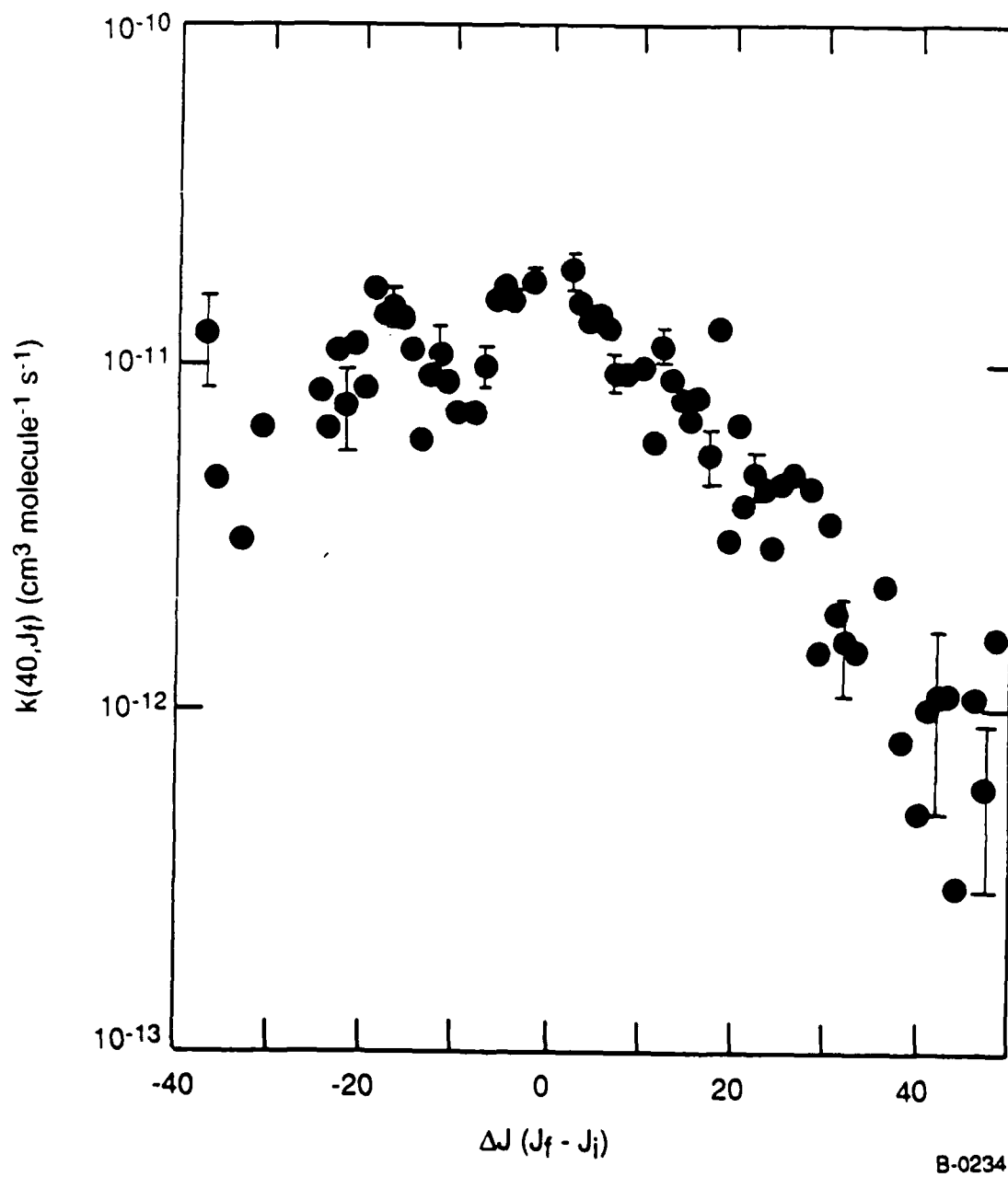


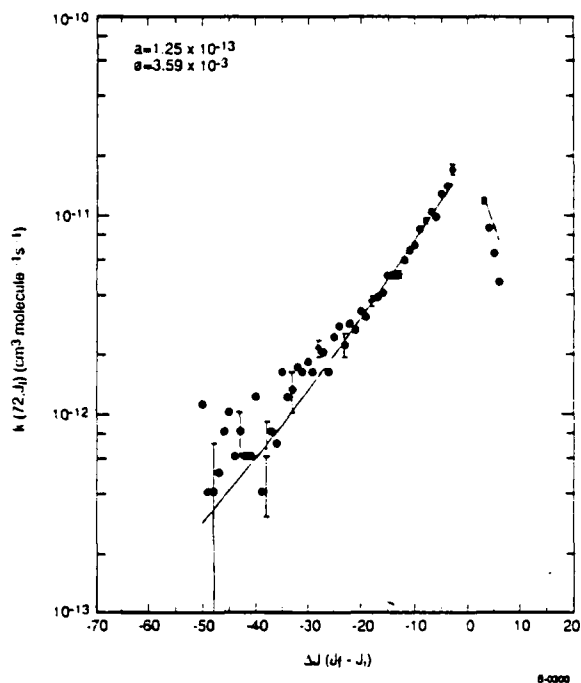
Figure 11. Preliminary Matrix of R-T Rate Coefficient for
ICl + He, $J_i=40$

It is also of interest to note that the rate coefficients for total R-T removal from $J_i=40$ are large $k_T^{Ar} = 5.9 \times 10^{-10} \text{ cm}^3 \text{ molecules}^{-1} \text{ s}^{-1}$ and $k_T^{Ne} = 5.8 \times 10^{-10} \text{ cm}^3 \text{ molecules}^{-1} \text{ s}^{-1}$. These values are about a factor of two higher than for IF. However, this might be accounted for by the fact that the rotational energy spacing in ICl(B) is less than half that of the respective spacing in IF(B). We also note that the total R-T rate coefficient in $I_2(B)$ are also considerably larger than in IF(B), but the rotational spacing in $I_2(B)$ is nearly a factor of ten less than that in IF(B). We will be making similar comparisons as we expand and better quantify our ICl data base.

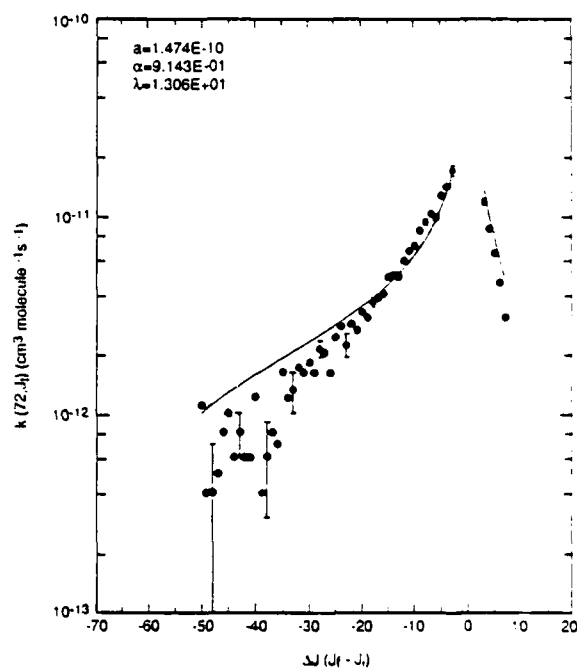
D. Fitting Law Analysis in IF(B)

We are comparing the four fitting laws described previously with particular emphasis on $J_i=72$ and some of these results are shown in Figures 12 through 14 using He, Ne, and Xe bath bases. Figures 12(a-d) show fits using the four laws for He, Figures 13(a-d) show similar comparisons for Ne, and Figures 14(a-d) show the same comparisons for Xe as the collision partner. We note that the simplest description, the energy gap law, is inferior to the other three fitting laws. Interestingly, the power gap law compares favorably with the angular momentum based laws. This same result was also observed by Pritchard and co-workers in $I_2(B)$.¹⁹ We will be extending these comparisons to the other bath gases in the next few months.

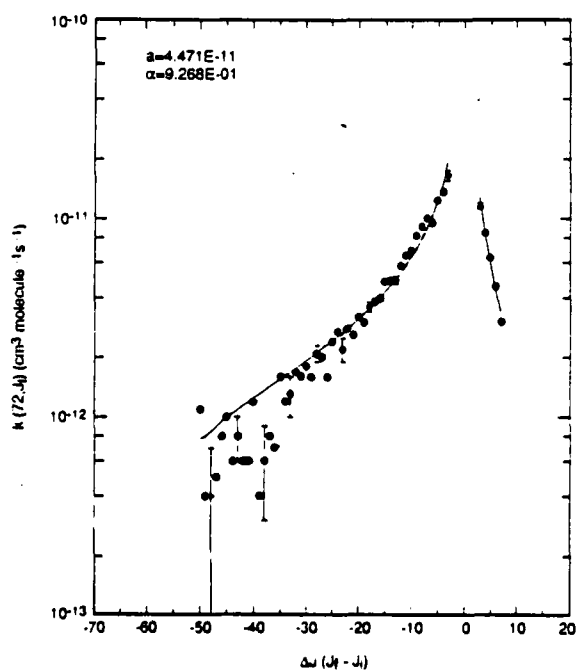
The predictive power of the scaling laws is of critical importance to incorporation of any law into a kinetic code that includes rotational energy transfer. We have begun to test these laws and present some preliminary results below. In Figure 15 we show data for R-T rate coefficients with helium where $J_i=27$. The solid line is the prediction of the IOS law using the parameters obtained from the $J_i=72$ data in Figure 12. In Figure 15 the solid line is not a fit to the $J_i=27$ data. Rather it represents the R-T rate coefficient for $J_i=27$ predicted from the parameters determined from the $J_i=72$ data. This is an extremely encouraging and exciting result.



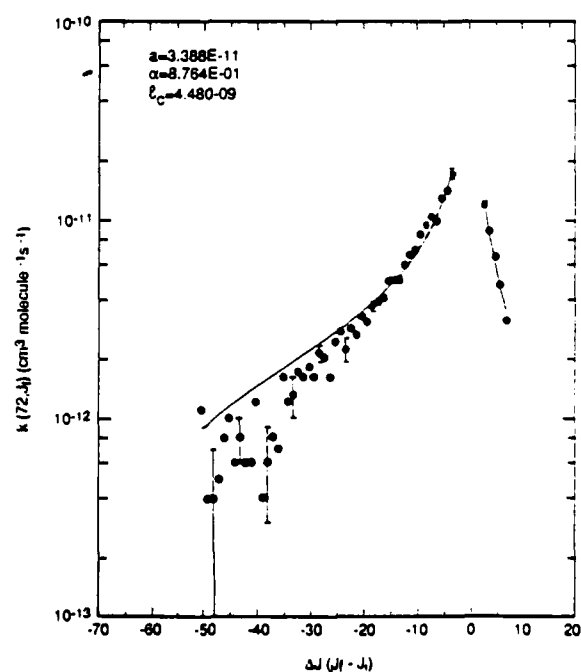
a)



b)

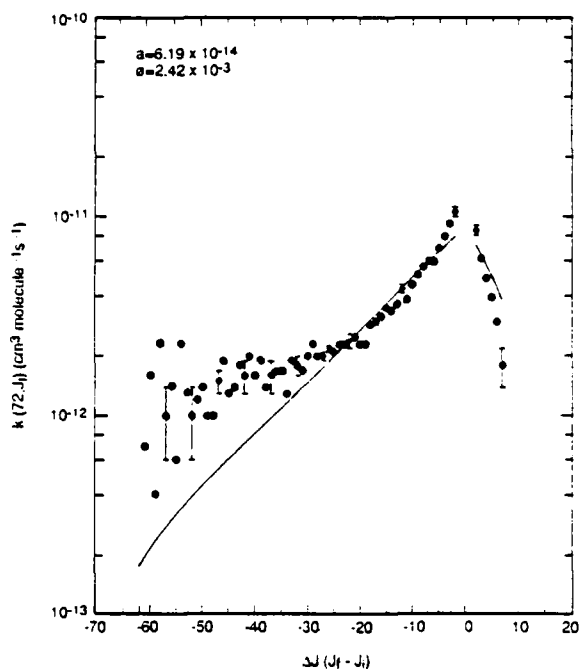


c)

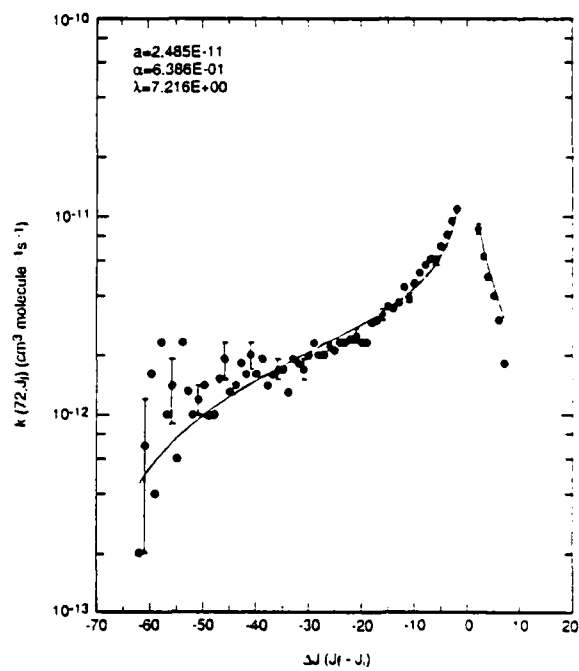


d)

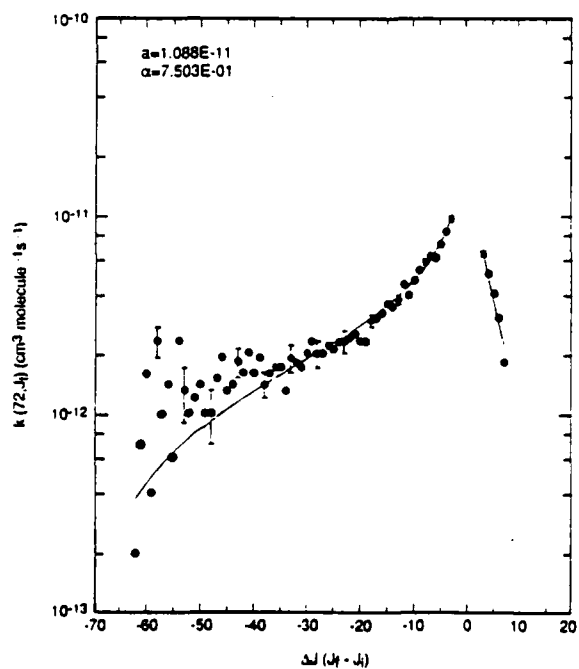
Figure 12. Comparisons of Four Fitting Laws to IF + He Data for $J_1=72$
a) EG Law, b) SPG Law, c) IOS Law, d) ECS Law



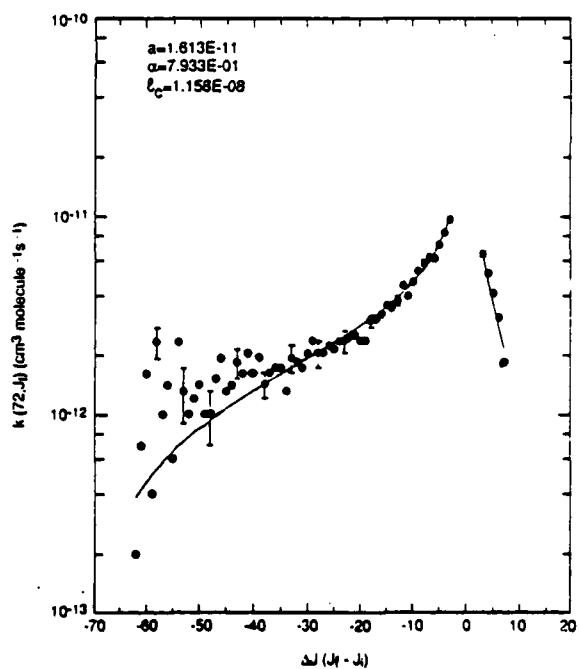
a)



b)

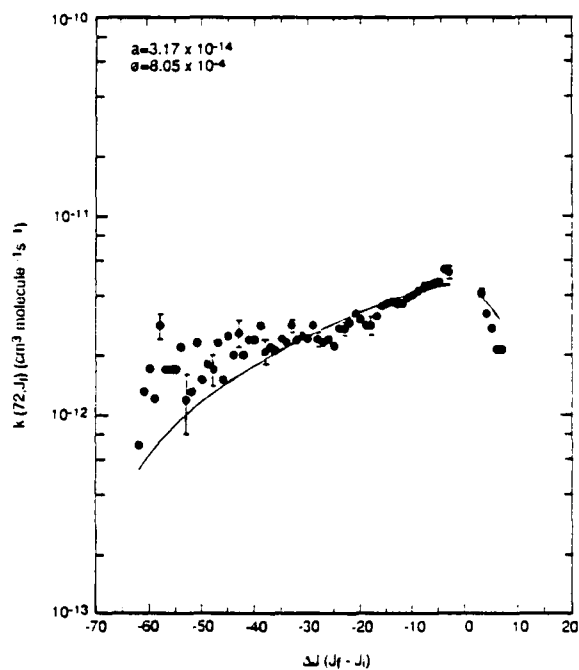


c)

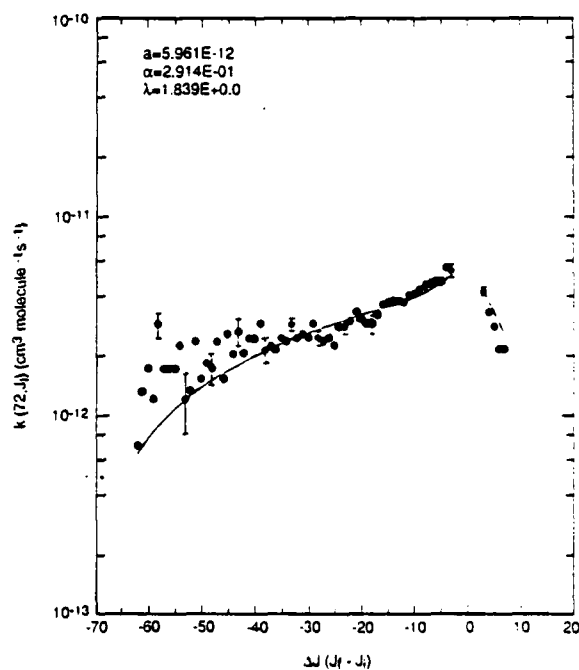


d)

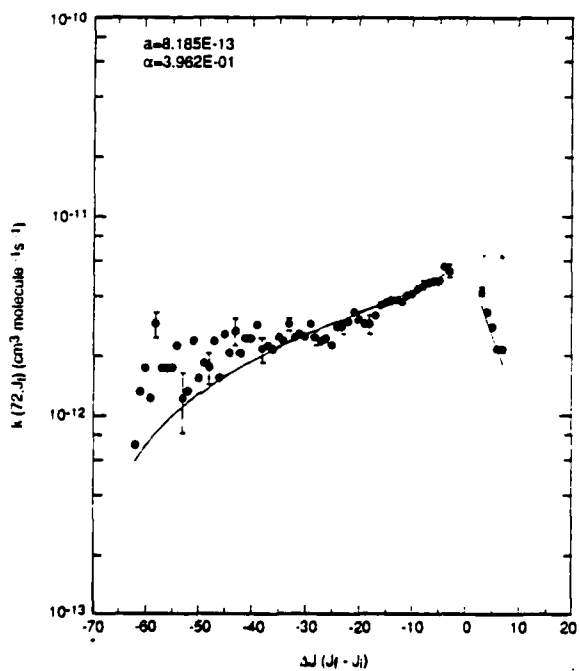
Figure 13. Comparisons of Four Fitting Laws to IF + Ne Data for $J_1=72$
a) EG Law, b) SPG Law, c) IOS Law, d) ECS Law



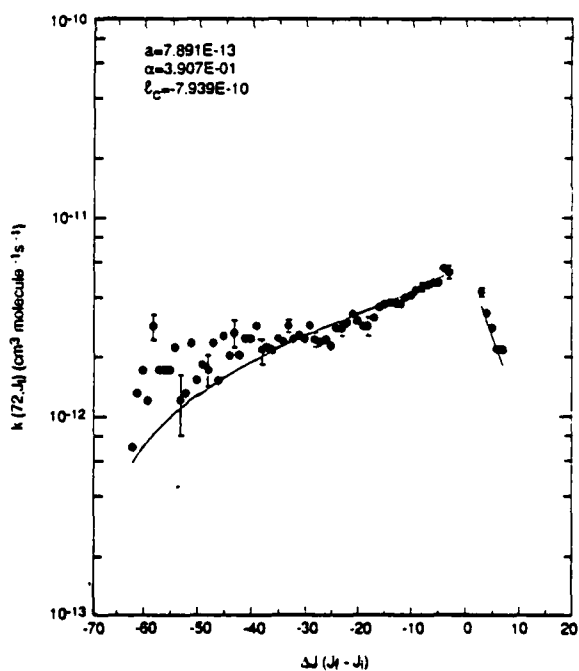
a)



b)

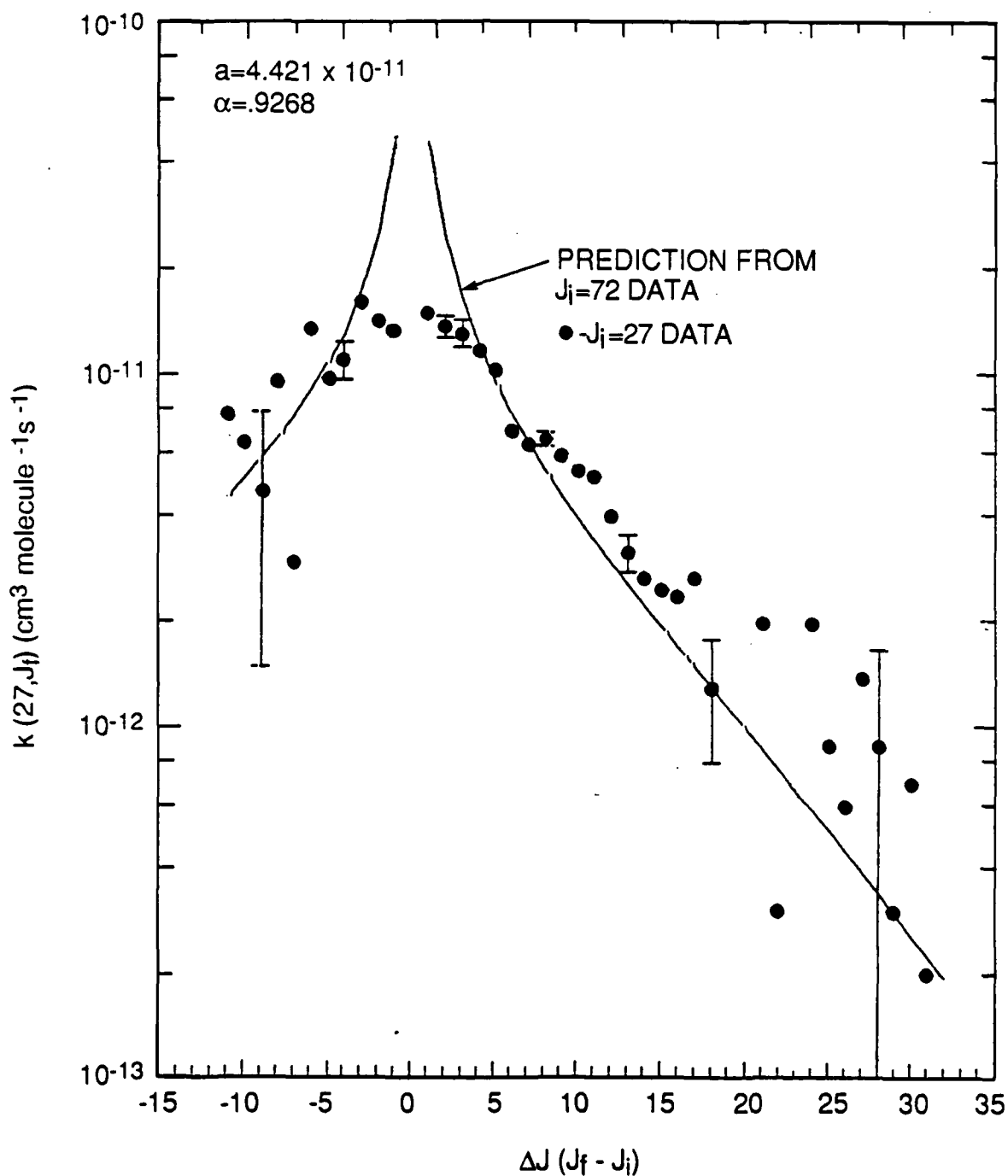


c)



d)

Figure 14. Comparisons of Four Fitting Laws to IF + Xe Data for $J_1=72$
a) EG Law, b) SPG Law, c) IOS Law, d) ECS Law



B-0314

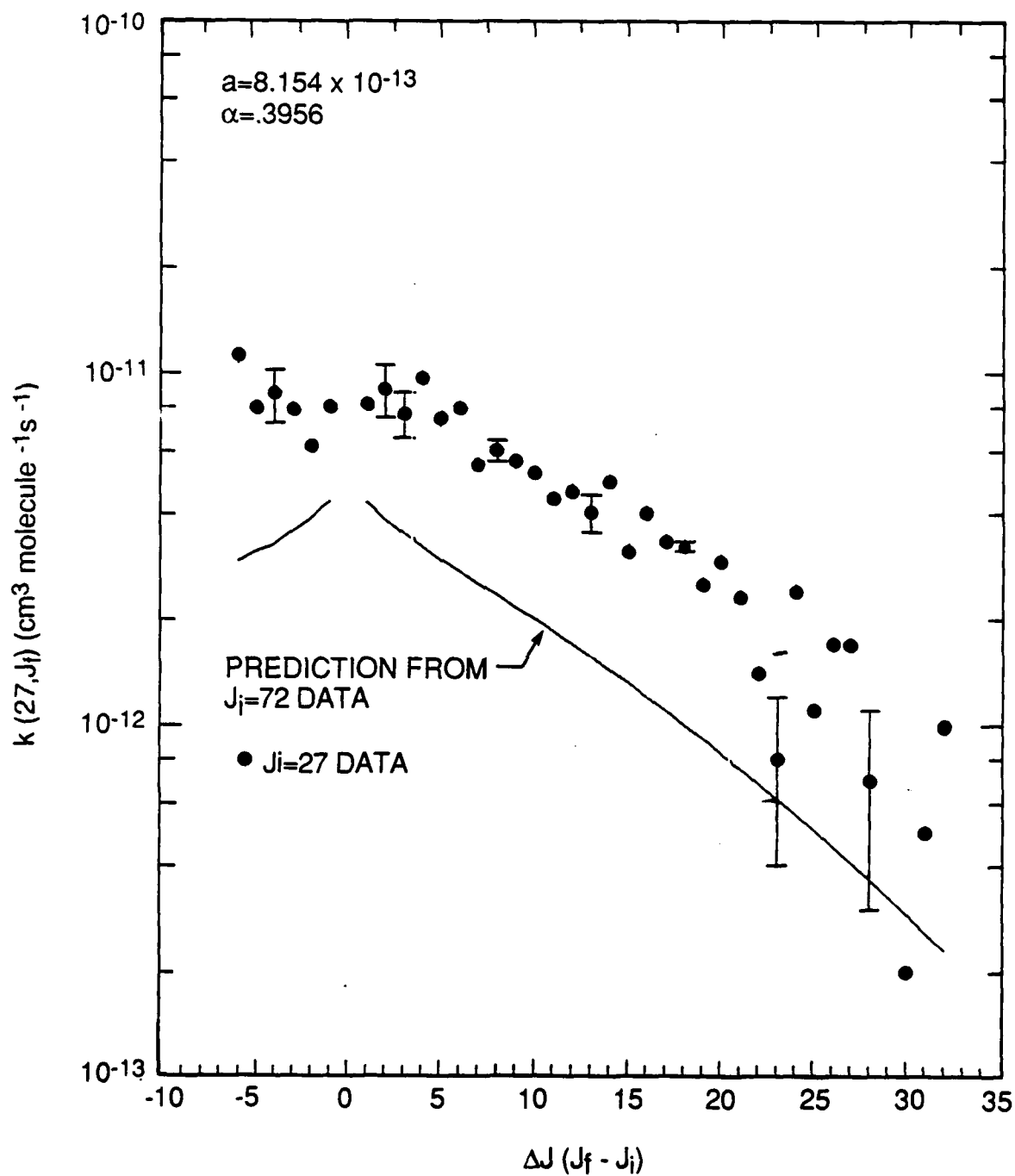
Figure 15. Comparison of Prediction of IOS Law to Data for IF + He, $J_i = 27$. Solid line is the prediction for $J_i = 27$ based upon parameters observed from $J_i = 72$ data.

A similar plot for $J_i=27$ with the collision partner Xe is shown in Figure 16. Although the parameters determined from the $J_i=72$ data underpredict the $J_i=27$ data by approximately 1.5, the fall off in the rate coefficient at large ΔJ is accurately predicted. Our approach to producing more accurate scaling laws parameters is to apply the fitting laws to the rate coefficients determined for each $J_i=13, 27, 35$, and 72 . We will then take an average for each fitting parameter to obtain global fitting parameters. This will be done for each collision partner. Finally we will use these global fitting parameters to predict rate coefficients for $J_i=13, 27, 35$, and 72 as a final test of the predictive powers of each scaling law.

Conclusions

We have presented a reasonably complete description of our results on IF(B). Several fitting laws have been applied to the several hundred IF R-T rate coefficients and we see that several fitting laws appear to provide a reasonably good description of the scaling of R-T rate coefficients as a function of ΔJ for the rare gas atom targets. Thus it appears that a closed form "generating function" of R-T rate coefficients can indeed be incorporated into existing or future IF chemical laser codes. During the next few weeks we will be completing our comparisons of the IF data set to these fitting laws.

The preliminary results on ICl(B) lead us to believe that we will be able to produce a similar data base for ICl which can then be compared to the same fitting laws and to the IF results.



B-0313

Figure 16. Comparison of Predictions of IOS Law to IF + Xe Data, $J_i=27$. Solid line is the prediction for $J_i=27$ based upon parameters derived from $J_i=72$ data.

REFERENCES

1. Steinfeld, J.I. and Ruttenberg, P., Scaling Laws for Inelastic Collision Processes in Diatomic Halogens, JILA Information Center Report, University of Colorado (1983).
2. Steinfeld, J., Rate Data for Inelastic Collision Processes in the Diatomic Halogen Molecules," J. Phys. Chem. 13, 445 (1984).
3. Davis, S.J., Rotational Energy Transfer in Metastable States of Heteronuclear Molecules, Physical Sciences Inc. PSI-1006/TR-830, June 1988.
4. Brunner, Timothy A. and Pritchard, David, Fitting Laws for Rotationally Inelastic Collisions, ed. K.P. Lawley, John Wiley & Sons, 589 (1982).
5. Marinelli, W.J. and Piper, L.G., "Franck-Condon Factors and Absolute Transition Probabilities for the IF ($B^3\Pi_0^+ \rightarrow X^1\Sigma^+$) Transition, JQSRT 34, 321 (1985).
6. Trickl, T., "Laserspektroskopische Untersuchungen an Jodmonofluorid, gebildet in den Reaktionen von Fluoratomen mit ICl, IBr und I_2 in gekreuzten Molekularstrahlen," MPI Quant. Inst. 71 (1983).
7. Trickl, T. and Wanner, J., "IF($A \rightarrow X, B \rightarrow X$) Chemiluminescence from the $F + I_2F$ Reaction," J. Chem. Phys. 74, 6508 (1981).
8. Clyne, Michael A.A. and McDermid, I. Stuart, " $B^3\Pi(0^+)$ States of IF, ICl, and IBr, Part 1 - Calculation of the RKR Turning Points and Franck-Condon Factors for the B-X Systems," JCS Faraday II 73 2242 (1977).
9. Kitamura, M., Kondow, T., Fuchitsu, K., Munakata, T., and Kasuya T., "Fluorescence Lifetimes and Spontaneous Predissociation of $I^{35}Cl(B0^+, v'=1$ and 2) as Studied by Laser Excited Fluorescence," Phys. Chem. Res., 1985.
10. Suzuki, T. and Kasuya, T., Predissociative Lifetimes of Single Rovibronic Levels of the $B^3\Pi_{0^+}(V'=3)$ State of ICl," 1984.
11. Polanyi, J.E. and Woodall, K.B., "Mechanisms of Rotational Relaxation," J. Chem. Phys. 56, 1563 (1972).
12. Pritchard, D.E., Smith, N., Driver, R.D., Brunner, T.A., "Power Law Scaling for Rotational Energy Transfer," J. Chem. Phys. 70, 2115 (1979).
13. Brunner, T.A., Smith, N., Dappr, A.W., and Pritchard, D.E., "Rotational Energy Transfer in $Na_2^*(A\Sigma)$ Colliding with Xe, Kr, Ne, He, H_2 , CH_4 , and N_2 : Experiment and Fitting Laws," J. Chem. Phys. 74, 3324 (1981).

14. DePristo, A.E., Augustin, S.D., Ramaswamy, R., and Rabitz, H., "Quantum number and energy scaling for nonreactive collisions," J. Chem. Phys. 71(2), 850 (1979).
15. Steinfeld, J.I, and Klemperer, W., "Energy-Transfer Processes in Monochromatically Excited Iodine Molecules: I. Experimental Results," J. Chem. Phys. 42(10), 3475 (1965).
16. Ottinger, C. and Schroder, M., "Collision-Induced Rotational Transitions of Dye Laser Excited $\text{Li}_2(\text{A}^1\Sigma_u^+)$ Molecules: Cross Sections and Their $+\Delta J/-\Delta J$ Asymmetry," J. Phys.^uB, 13, 4163 (1980).
17. Crosley, D.R., "Energy Transfer in $\text{A}^2\Sigma^+ \text{OH}$. I. Rotational," J. Chem. Phys. 67, 2085 (1977).